Investigation of multi-lobed fighter jet noise sources using acoustical holography and partial field decomposition methods[1]

Alan T. Wall[2]
Air Force Research Laboratory, Wright-Patterson Air Force Base, OH 45433, USA

Kent L. Gee,[3] Tracianne B. Neilsen,[4] and Blaine M. Harker[5]
Brigham Young University, Provo, UT 84602, USA

Sally Anne McInerny[6]
University of Louisiana, Lafayette, LA 70504, USA

Richard L. McKinley[7]
Air Force Research Laboratory, Wright-Patterson Air Force Base, OH 45433, USA

and

Michael M. James[8]
Blue Ridge Research and Consulting, Asheville, NC 28801, USA

Full-scale tactical aircraft noise exhibits multiple radiation lobes not seen in laboratory-scale jets. These lobes have different radiation directions yet appear to have similar, overlapping source regions. Near-field acoustical holography (NAH) source reconstructions, in conjunction with partial field decomposition (PFD) methods that produce physically meaningful partial fields, are used in the current work to investigate the nature of these radiation patterns. First, it is shown that the two main radiation lobes are highly incoherent, suggesting independent partial sources. Second, these lobes are isolated as mutually orthogonal partial fields. In this representation, the lobes seem to be generated by independent yet spatially coincident extended partial sources. Source comparisons are made between non-afterburner and afterburner engine powers to investigate whether afterburner combustion produces any sources that are fundamentally different from those of non-afterburner operations. The current results show no qualitative changes occur due to the addition of the afterburner thrust aside from minor variations in source distribution, level, and the nature of the overlap between the multiple lobes.

---

[1] Distribution A: Approved for public release; distribution unlimited. 88ABW Cleared 04/09/2015; 88ABW-2015-1837.

[2] Corresponding Author, Postdoctoral Fellow, Battlespace Acoustics Branch, 2610 Seventh St., Bldg. 441, Wright-Patterson AFB, OH 45433, AIAA Member.

[3] Associate Professor, Dept. of Physics and Astronomy, N283 ESC, Provo, UT 84602, AIAA Senior Member.

[4] Part-time Professor, Dept. of Physics and Astronomy, N283 ESC, Provo, UT 84602.

[5] Graduate Student, Dept. of Physics and Astronomy, N283 ESC, Provo, UT 84602, AIAA Student Member.

[6] Professor and Department Head, Dept. of Mechanical Engineering, University of Louisiana, P.O. Box 44170, Lafayette, LA 70504.

[7] Principal Acoustics Engineer, Battlespace Acoustics Branch, 2610 Seventh St., Bldg. 441, Wright-Patterson AFB, OH 45433.

[8] Vice President and Senior Principal Engineer, 29 N Market St., Suite 700, Asheville, NC 28801, AIAA Member.

Nomenclature

AB   =   afterburner engine power
MIL   =   military engine power
x,y,z =   Cartesian coordinates with respect to the aircraft nozzle location
θ =   radiation angle with respect to jet engine inlet axis

I. Introduction

ALTHOUGH many properties of full-scale jets have been reproduced in laboratory-scale jets, such as characteristic spectral shape and source directivity,[1] jets on tactical fighter aircraft exhibit some unique characteristics, such as a lack of clear evidence of broadband shock-associated noise in the one-third-octave (OTO) spectra at sideline angles, shallower high-frequency spectral slopes than lab-scale data, and spectral shapes typical of fine-scale turbulence in the far downstream region.[1-3] In particular, the appearance of multiple peaks in the acoustic far-field spectra of the jet mixing noise is predominantly a characteristic of full-scale tactical jets.[1-9] The acoustical nature of the radiation lobes that generate these peaks is the focus of the current paper.

A double peak has been seen in ground run-up spectra of several tactical jet aircraft, including the F/A-18E/F,[4,5] the F-35AA-1,[6] the F-35A and F-35B,[10] the F-22A,[2,3,7] the uninstalled engine for an F/A-18C/D,[11] the uninstalled General Electric YJ97-GE-3 engine used on a high-altitude reconnaissance drone,[11] and in measurements of an unspecified supersonic exhaust engine with a round nozzle and capable of afterburner (AB) operations.[1] It was present in the flyover noise spectrum of the F-15 ACTIVE[8] and in an additional flyover test of an unspecified aircraft.[9] In the case of the F-22A and the F-35AA-1, Neilsen *et al.*[3,12,13] showed that the popular two-source similarity spectra[14] could not account for the double spectral peak. In an effort to explain this phenomenon for the F-22A, Tam and Parrish[15] related the different spectral peaks to combustion noise and the passage of "hot spots" through a pressure discontinuity at the nozzle throat caused by a change from the converging to the diverging nozzle portions (entropy waves). Turbulent flow and combustion data are not yet available to corroborate or refute these claims about jet acoustic source mechanisms, but several acoustic imaging techniques have shown F-22A source distributions centered on regions well downstream of the nozzle.[7,16,17] In addition, the supersonic engine tested by Schlinker *et al.*[1] did not exhibit an increase in noise from the nozzle exit region in the direction of maximum radiation with the addition of fuel.

The predominance of each spectral peak varies with downstream location when measured along the extent of the F-22A jet mid field, such that there is not only a double peak in the spectrum at certain locations, but there is also a double peak in the spatial sound pressure level (SPL) distribution at certain frequencies.[3,18] Stout *et al.*[19] showed that the double peak phenomenon also occurs in the spatially distributed vector intensity field of the F-22A. They demonstrated that low coherence exists between the two spatial peaks,[16] which suggests that the noise generation mechanism produces independent radiation lobes. In a direct attempt to model source behavior that leads to this double peak, they modeled the source with two mutually incoherent, yet overlapping, distributions and matched their radiated intensities to the measured intensity distribution. Fisher *et al.*[20] show similar behavior in the low-Strouhal-number noise source reconstruction of a Rolls-Royce Viper 601 engine, which was reconstructed using the polar correlation technique. They showed a phase discontinuity in the jet source reconstruction between two distinct peaks, suggesting that the two peaks might be independent. They also found a phase discontinuity in the reconstruction of a laboratory-scale jet, but the limited resolution of the reconstruction technique precluded any distinction between peaks in the magnitude distribution. Nevertheless, this study demonstrated that incoherent source mechanisms might be possible in laboratory scale jets, even if they do not result in a double-peak spectrum.

F-22A source reconstructions[7,17] have also been obtained through advanced beamforming[21] and near-field acoustical holography (NAH)[22,23] methods. Both reconstructions suggest that two or more overlapping source regions generate radiation lobes that point in different directions, resulting in multiple spatial/spectral peaks in the field. It is desirable to know, *Are the sources of the multiple lobes coherent or incoherent radiators?* The low mutual coherence in the field, shown by Stout *et al.*,[16] supports the idea of incoherent sources. Harker *et al.*[24] showed the same low mutual coherence between the two peak regions at 200 Hz with the engine operating at military (MIL) power. They also used cross-correlations across a linear microphone array to show evidence of F-22A noise signals arriving at the array with two different phase speeds (or trace velocities) along the array. Such a phenomenon could be caused by compact sources in different locations, or extended sources with different convective velocities (phase speeds). Because jet mixing sources are extended sources that grow to peak amplitude followed by gradual decay, it is possible that a combination of these two ideas approaches the truth. The partial field decompositions (PFDs) of the F-22A at MIL power and at 400 Hz[25] showed that a single wide lobe could be represented as the superposition of several narrow mutually incoherent lobes with variable source origins and directionalities. In the current study,

spatial coherence between the two distinct lobes is investigated. In addition, the PFD method of partial coherence decomposition (PCD)[26] is used to isolate the two lobes into mutually incoherent partial fields (PFs).

The PCD method is one of several PFD methods that can be used in jet noise studies. The theory of PFD is based on principal component analysis, and is used to investigate the most energetic portions of stationary random sources. All PFD methods produce mutually orthogonal PFs, but the PFs are not unique. For example, singular value decomposition (SVD)[27,28] is a useful PFD method for determining a minimum number of partial fields required to represent an unknown number of sources. However, PFD methods do not generally result in physical meaningful PFs, i.e., PFs that can each be related directly to independent source mechanisms.[26] The PCD method approaches a physically meaningful isolation of independent sources, or "partial sources." In PCD, a set of reference microphones are placed in the field such that they collectively detect the signals from all partial sources. An LU eigenvalue decomposition based on Cholesky factorization[29] of the cross-spectral matrix of the reference signals forms a basis for the PF generation. This type of decomposition is a noise-rejection method; the eigenvectors are ordered such that all field information coherent with the first reference is included in the first PF and excluded from all others, the field information coherent with the second reference is exclusive to the second PF, and so on. Thus, the order of reference selection affects the PFs. In an idealized scenario, the partial source signals would serve as the reference signals. Since actual partial source signals (without cross-talk) are difficult to measure in practice, reference signals that are strongly related to source signals are sought. When reference microphones are placed such that each one is dominated by the signal from a single source (usually obtained by placing each reference microphone near a source and far from all others) the resulting PFs approach a representation of partial sources. If the reference cross-spectral matrix is nearly diagonal, this indicates a well-selected set of references. Successful source isolation depends on how exclusive (incoherent) the reference signals are. When the locations of sources are unknown, the multiple signal classification (MUSIC) algorithm[30] can be used to select an optimal subset of references from a larger candidate set placed around the source region.[26]

Three-dimensional field reconstruction with NAH offers a method to isolate partial sources further when used in conjunction with PCD. In general, NAH uses a measurement of complex pressures over a two dimensional surface (the hologram) to predict (reconstruct) the three-dimensional wave field in the vicinity of the array, including reconstructions of the source. One NAH approach is to calculate the spatial discrete Fourier transform of the hologram pressures to represent the surface in the wavenumber domain, apply a wave propagation model to a new parallel surface, and perform the inverse Fourier transform to recover the sound field.[22] Alternatively, the three-dimensional sound field may be represented as a superposition of elementary wave functions, and an optimized fit of these functions to the measured hologram data may be calculated.[23] Since NAH requires a coherent hologram input, in the case of multiple independent sources it is common practice to perform PFD first, apply NAH to reconstruct the source components of each PF independently, and then sum the reconstructions to obtain the final source.[28] Holographic methods were used to reconstruct source distributions and radiated fields of laboratory jets,[31-33] and they have been adapted for use on the full-scale jet of the current study.[7,34]

An advantage of NAH is that reconstruction of complex PFs provides an estimation of the three-dimensional cross-spectra. Thus, after NAH, a "virtual reference" (VR) can be placed anywhere in the reconstructed field as if a physical reference had been present. Then, the field can be re-decomposed into a new set of PFs based on the new VR signals.[35] Kim et al.[36] showed that the methods of VR generation using NAH could be combined with the MUSIC algorithm to find optimal VR locations. Wall et al.[37] modified this method for use with an unknown number of sources and produced the F-22A PFs shown in Ref. [25].

In the current paper, instead of seeking an optimal VR placement, VRs have been placed deliberately in the peak regions of the F-22A radiation lobes. Although the conventional approach is to place references close to sources, aeroacoustic sources present a unique challenge; jet mixing noise is comprised of extended sources with spatially decaying coherence and little to no spatial separation. However, the directional multilobe nature of the F-22A field presents a unique alternative. It is shown here that the two primary lobes are independent, confirming the low mutual coherence shown by Stout et al.[16] and Harker et al.[24] Hence, the placement of VRs in the respective lobe maxima in the far field results in PFs that isolate the lobes. These PFs are investigated for insight into the partial sources and their radiation properties.

Reconstructions of F-22A Raptor noise fields were obtained in a previous study[7] using multisource statistically optimized near-field acoustical holography (M-SONAH).[23] For the current investigation, PCD of these reconstructed fields has been performed based on VRs in the far-field regions of distinct lobe maxima. These methods have been used to obtain (1) field coherences with respect to each lobe, (2) physically relevant partial fields, and (3) a comparison of source properties between non-afterburner and afterburner engine operations. Section II of this paper provides a summary of the experimental setup. Section III gives a description of the NAH and PCD processing. Section IV shows a subset of NAH reconstructions of the field, the selected VR locations, spatial coherence of the

3

field with respect to the VRs, and the resulting partial fields and partial sources. Two engine powers, MIL and AB, are shown in order to understand the effects of added thrust from AB operations. For both engine powers, the frequencies 200 Hz and 315 Hz are the focus of the investigations, because these frequencies exhibit the greatest distinction between the multiple lobes. In Section V, conclusions are discussed and an explanation is provided for how alternative VR selections could be used to investigate mutually incoherent jet sources that do not generate discrete lobes.

II.   Experiment

Researchers from Blue Ridge Research and Consulting and Brigham Young University conducted static run-up tests in 2009 on the Lockheed Martin/Boeing F-22A Raptor at Holloman Air Force Base, New Mexico.[18] The two Pratt & Whitney F119-PW-100 turbofan engines on the F-22A each have a rectangular nozzle aspect ratio of about 2:1, which is complicated by the presence of movable thrust vectoring paddles. The center of each nozzle was 1.9 m (75 in) above the ground. With the aircraft tethered to a run-up pad, the engine nearest the measurement arrays was cycled through several engine powers while the other engine was held at idle. The concrete run-up pad was 24.4 m (80 ft) wide with rain-packed dirt on either side. The dominant source of reflections in the jet vicinity was the run-up pad.

The F-22A experiment is the most extensive near-field measurement of a jet on a high-performance military aircraft to date. Figure 1 shows a schematic of the measurement. The origin of the coordinate system is on the ground directly below the nozzle exit. The holography array consisted of 90 microphones with two-dimensional regular spacing of 0.15 m (6.0 in). The planar hologram surface consisted of 30 "scans" and was aligned so as to be parallel to the estimated shear layer boundary. In order to generate a coherent hologram from the incoherent scans, 50 reference microphones were placed along the ground, parallel to the jet centerline, at $x = 11.6$ m, with regular 0.61-m (2-ft) spacing. Additional details about the experiment setup were provided by Wall *et al.*[18]
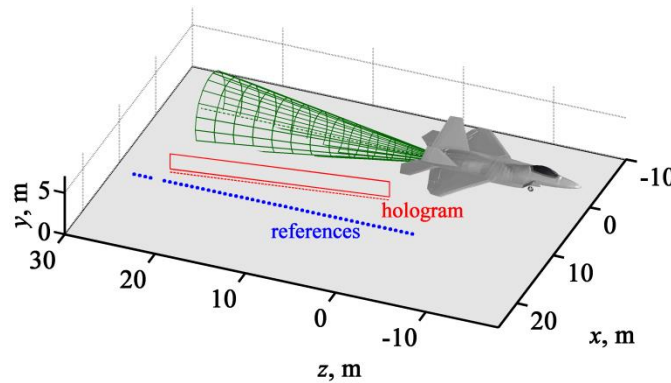
Figure 1. NAH measurement schematic for the F-22A Raptor experiment.
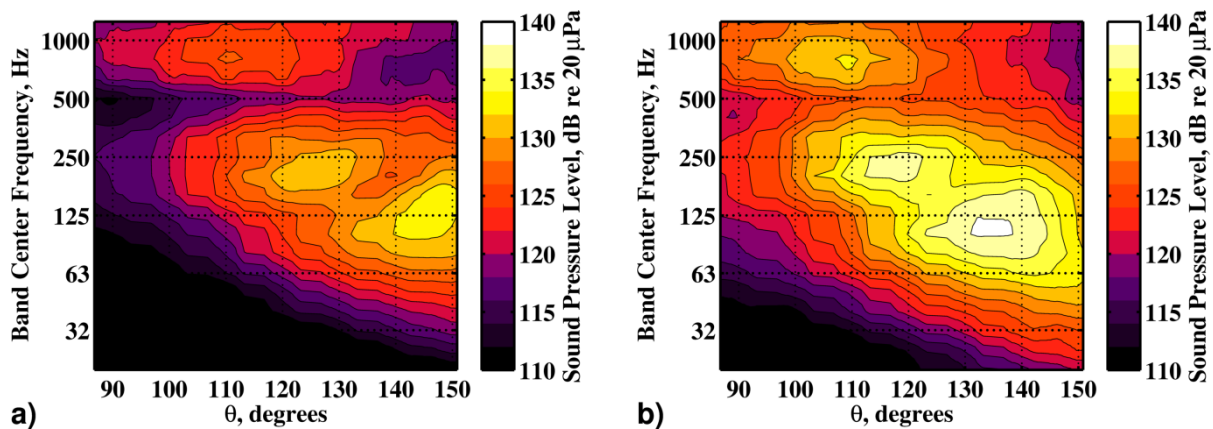
Figure 2. Measured OTO spectra along the arc, at a height of $y = 1.9$ m, for (a) MIL and (b) AB power. Contour lines are separated by 2 dB.

4

American Institute of Aeronautics and Astronautics

Figure 2 shows the measured OTO spectra along the row of the arc that is the same height as the nozzle centerline ($y = 1.9$ m) for MIL and AB powers. The angle θ is defined with respect to the jet inlet axis, and the arc measurement was centered on the point 5.5 m downstream of the nozzle exit, which is near the maximum source region. The nulls near 500 Hz are due to destructive interference from ground reflections. However, note the presence of two distinct maximum regions in the spatial/spectral map between about 125 and 250 Hz for both powers. The shallower nulls between these two points are not due to destructive interference—the same nulls occur in the measurements made by the ground-based reference array.[12,18] These are the multiple peaks investigated here.

III. Methods

The process for obtaining the PFs is summarized as follows.

1. Use an SVD of the physical reference cross-spectral matrix to perform a preliminary PFD.
2. Numerically extend the PF apertures.
3. Reconstruct the field using M-SONAH.
4. Select VR locations (lobe-centered in this study).
5. Perform PFD using the PCD of the VRs.

Each step is described with additional details below.

First, in order to produce coherent holograms from incoherent scans, a preliminary PFD has been performed on the measured data using an SVD of the physical reference cross-spectral matrix, according to the methods of Lee and Bolton.[31,38] Second, the PFs have been numerically extrapolated in the forward and aft directions to mitigate the effects of the aperture edges on field reconstructions.[7] Third, since the measurements were made in the presence of a rigid ground reflection, M-SONAH[23] has been used to reconstruct the field.[7] In this technique, the sound field is represented by a superposition of two sets of cylindrical wave functions, one centered on the jet centerline, and a second set centered on the reflected image of the jet. Wall *et al.*[7] recently performed a validation of this method by a comparison of benchmark measurements and sound field reconstructions for four engine powers and frequencies between 20 Hz and 1250 Hz. Field reconstructions for frequencies between 125 Hz and 400 Hz are shown here in Section IV for MIL and AB powers.

The two lobes are most distinct in the MIL case at 200 Hz and 315 Hz, and in the AB case at 200 Hz, so these cases are investigated. The lobes cannot be distinguished for the AB 315-Hz case, but this case is also investigated here for completeness. For the fourth step, two VR locations have been selected in the far field region centered on each lobe. It is understood that the ideal implementation of PCD requires the number of references to be equal to the number of sources.[36] If more references than sources are used, the reference cross-spectral matrix includes noise components and is therefore not full rank, causing instabilities in the matrix inversion during PCD processing. If too few are used, the matrix will be full rank, but the basis vectors will not be complete—not all energy in the field will be represented in the PFs. In the case of aeroacoustic sources, the number of sources is tenuous,[31,39] but methods have been developed to guide the design of a sufficient physical reference array.[40] In past studies, methods such as the virtual coherence technique[41] were used to in conjunction with SVD-based PFD to determine a practical number of singular values to include, which can be related to an effective number of jet sources.[31] However, in the current study, the number of VRs has deliberately been limited to the two in the visible lobe regions in order to investigate the specific source and field properties that are coherent with these lobes.

In the final step, the VR signals have been decomposed using Cholesky factorization[29] to form a linearly independent basis. The three-dimensional reconstructed field has been re-decomposed (projected onto the new basis)[36] to obtain the PFs shown here.

It is important to understand that an NAH reconstruction contains an estimate of the field cross-spectral information. Spatial coherence can be calculated from cross spectra,[42] and PCD based on VR signals relies on the cross spectra between each field point and the VRs. Although it is not a necessary step in the PCD process, spatial coherences have been calculated with respect to the VR points in order to investigate the relationships between lobes.

IV. Results

In Fig. 3, the MIL and AB reconstructions are shown as a function of aft distance, z, and distance from the jet centerline, x, at a height of $y = 1.9$ m. All OTO band center frequencies from 125 Hz to 400 Hz are shown. Levels have been scaled to represent the energy of the full OTO band. All levels are shown on the same color scale, 110 dB

to 140 dB, with contour lines separated by 2 dB. For all cases, the regions of local maxima form lobes that point aft, or in a direction that may be approximated by a large angle with respect to the jet inlet axis.

For MIL power shown in Fig. 3a, at 125 Hz, the radiation points toward about 155°. As frequency increases, the radiation shifts toward smaller angles, reaching about 120° at 400 Hz. A similar effect is seen in the AB data in Fig. 3b, but the radiation angles range from about 125° to 115° from 125 Hz to 400 Hz, respectively. A careful inspection of the contour patterns at small x values shows that higher frequencies also tend to originate from farther upstream than lower frequencies. Since source phase speed may be linked directly to radiation directivity,[43] and since jet flow is known to slow with distance downstream,[44] it has been postulated that convection velocity local to the maximum source region is the main influence on directivity.[7] Sources that originate farther downstream have lower characteristic phase speeds, and thus radiate at larger angles. A frequency-by-frequency comparison of the lobes between MIL and AB powers shows that directionality also tends to shift toward smaller angles with increasing engine power, consistent with the directivity dependence on convection velocity.
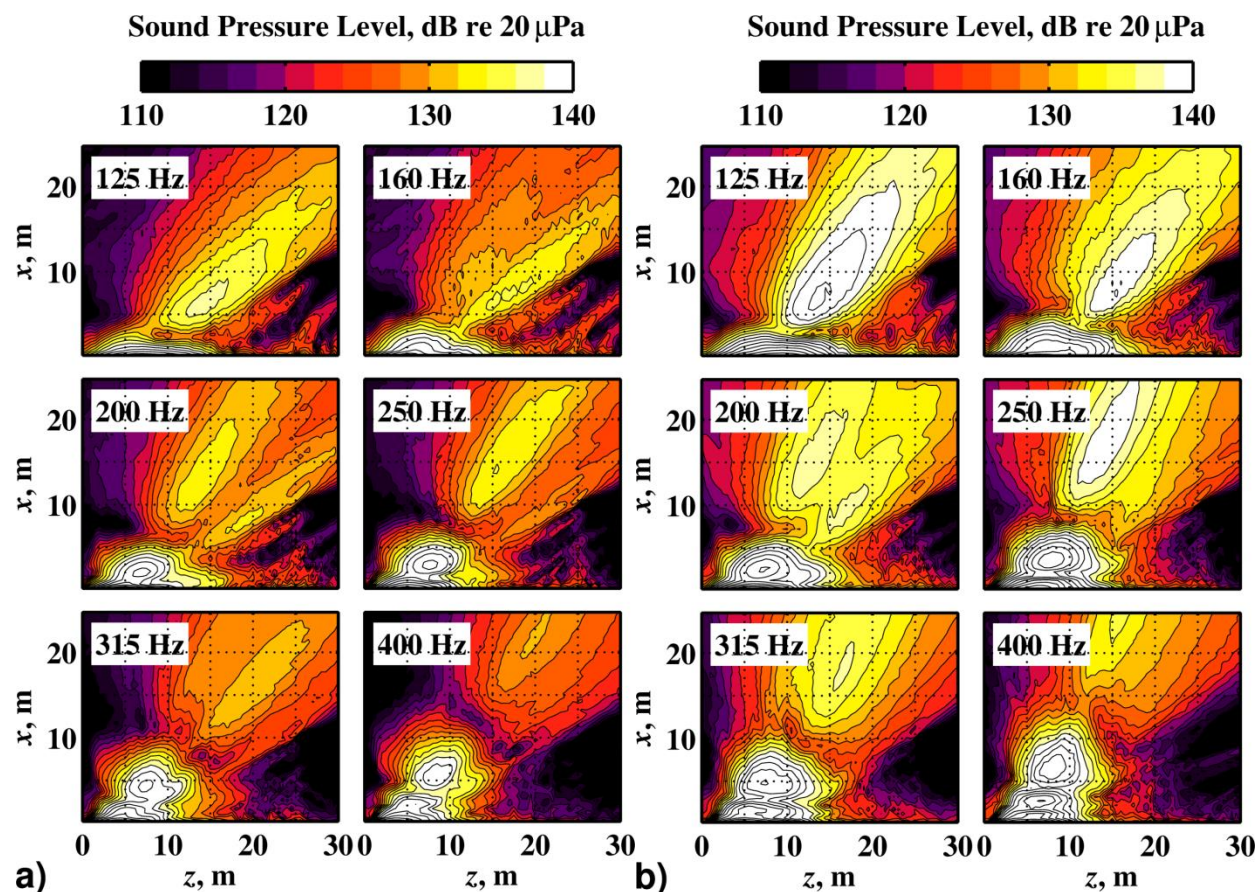
Figure 3. Reconstructed sound fields for OTO frequencies from 125 to 400 Hz, (a) MIL and (b) AB powers. Band-center frequencies are shown in the upper left corners of each field. Contour lines are separated by 2 dB.

Note the 200-Hz field for AB power in Fig. 3a. The contour lines show a shallow null region (roughly 5 dB down) running from the mid to the far field between two regions of locally high amplitudes. Similar distinct lobes can be seen for MIL at 160 Hz, 250 Hz, and to some extent 315 Hz in Fig. 3b, c, and d, respectively. For AB, the lobes are best distinguished at 200 Hz in Fig. 3b. These lobes result in the distinct maximum regions of Fig. 2. An inspection of these fields for low x values shows that the null cannot be seen in the near field; the lobes tend to originate from overlapping source regions but radiate in different directions. This demonstrates the difficulty in placing VRs near partial sources.

Reconstructions for 200 Hz and 315 Hz for both MIL and AB engine powers are shown in Fig. 4, this time over a polar arc out to 100 (equivalent) nozzle diameters. Figure 4a shows that the angles of the MIL 200 Hz lobes are about 20° different, so the lobes have an increasing spatial separation with distance from their origin. In each of the

American Institute of Aeronautics and Astronautics

other cases in Fig. 4, the angles separating the two lobes are smaller, about 15° or less, so the lobes are less distinct than in the MIL 200 Hz case.
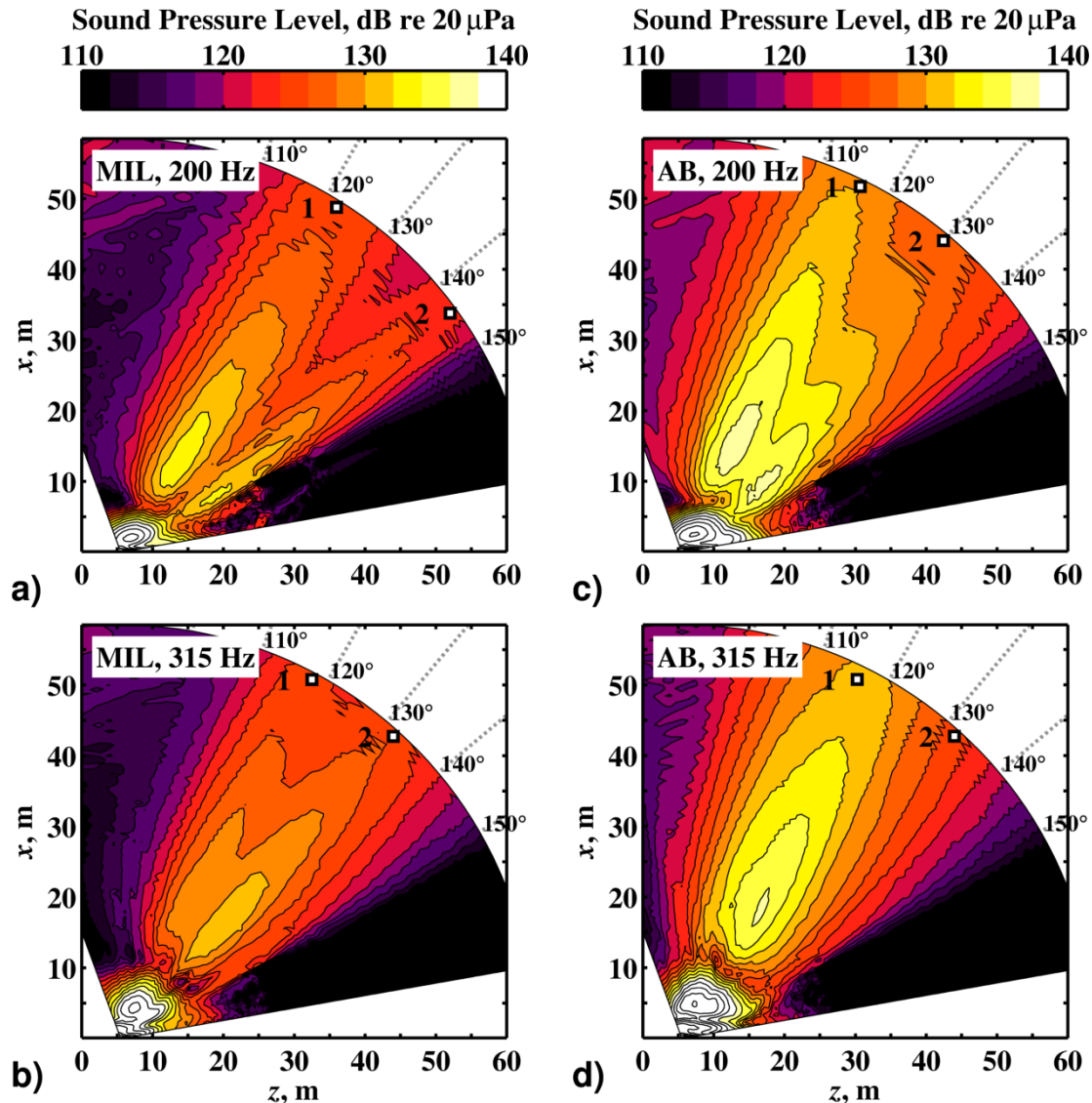
Figure 4. M-SONAH reconstructions out to approximately 100 nozzle diameters for (a) MIL 200 Hz, (b) MIL 315 Hz, (c) AB 200 Hz, and (d) AB 315 Hz. VR selection points are specified by squares. Contour lines are separated by 2 dB.

The VRs have been placed at the centers of each lobe near 100 nozzle diameters. Their locations are marked by the numbered squares in Fig. 4. Since the MIL 200 Hz field has the most distinct lobes, VR placement is straightforward. For MIL 315 Hz and AB 200 Hz, the lobes are separated by nulls that are only about 2 dB below the maximum lobe levels, but this is enough to visualize two distinct lobe maxima. It might be expected that shallower nulls between the two VRs would indicate more cross-talk, but this will be refuted by the coherence results below. (In this paper, the term cross-talk refers to shared source information detected by the VRs in the field, rather than an erroneous leakage of signal information in the measurement electronics.) Lastly, for the AB 315 Hz case, no second lobe can be distinguished. Thus, VR 1 was placed in the center of the primary lobe, and VR 2 was placed (somewhat arbitrarily) farther aft, such that there was low mutual coherence between the VRs, as shown below.

The coherence of each field with respect to its corresponding VRs are shown in Fig. 5 for MIL power. A coherence map is shown for each frequency and referenced to each VR, as indicated in the upper left corners of each

American Institute of Aeronautics and Astronautics

map. Regions of higher coherence are shown with darker colors. The first feature of interest is that, for all cases shown in Fig. 5, regions of high coherence extend from the near field (low values of x and z) out toward 100 nozzle diameters in the directions of the lobes, but are narrow in the direction perpendicular to propagation. (The noisy regions of high coherence far from the lobes are artifacts of the NAH processing and exist outside the region of valid reconstructions as explained by Wall *et al.*[7]) This demonstrates that the lobes are highly self-coherent, but the field outside of each lobe is generated by other independent sources.
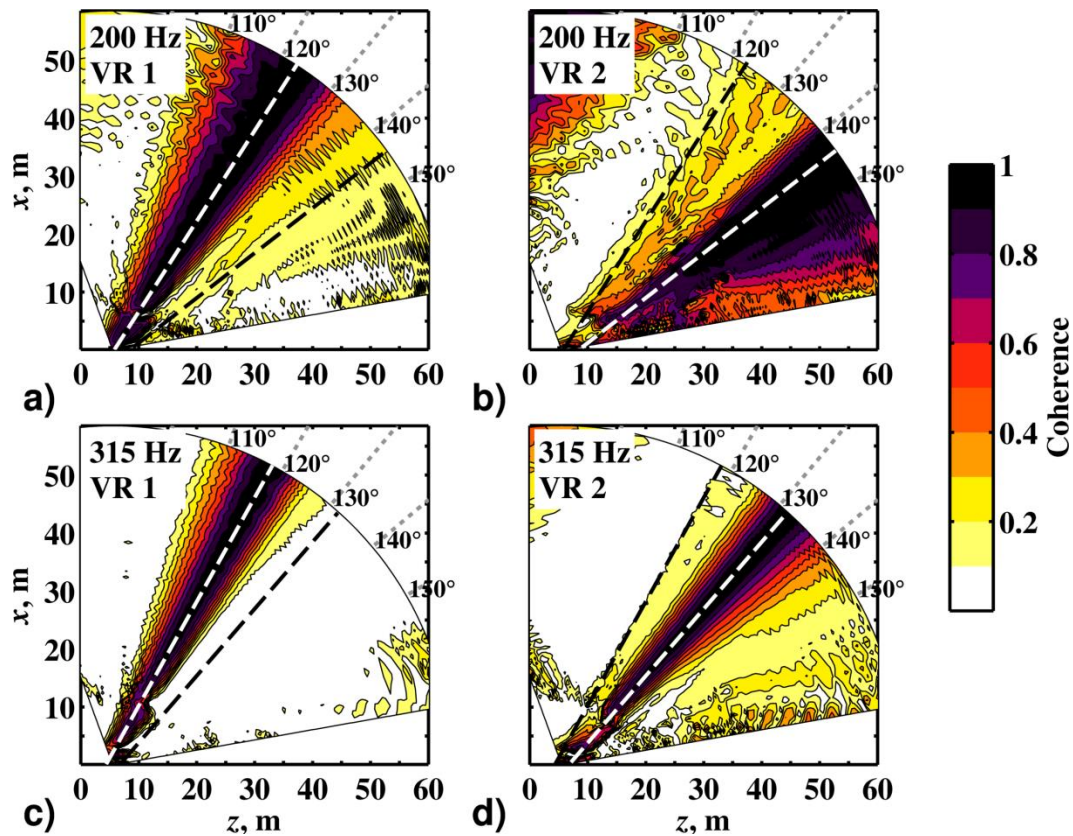
Figure 5. Coherence with respect to the selected VRs, MIL power. Band center frequencies and VR numbers are shown in the upper left corners of each field. Contour lines are separated by values of 0.1. Dashed lines are placed in identical locations between left and right figures to provide a spatial reference.

Dashed lines are added to each map in Fig. 5 for reference. For example, the white dashed line of Fig. 5a marks the region of high coherence for the MIL 200-Hz lobe 1. Its location coincides with the black dashed line of Fig. 5b. Thus, the coherence values marked by the black line indicate the portion of energy in the region of lobe 1 that is coherent with lobe 2. Similarly, the black line of Fig. 5a indicates the portion of energy in the lobe 2 region that is coherent with lobe 1. Since both of the black lines mark regions of nonzero coherence, there is some cross-talk—each VR detects some information from the opposite lobe. Similar lines are added to the MIL 315 Hz coherence maps of Fig. 5c and d. However, note that the coherence along the black line of Fig. 5c is practically zero. There seems to be less cross-talk at 315 Hz than in 200 Hz, even though the 200-Hz lobes are farther apart in space (compare Fig. 4a to Fig. 4b). Thus, lobe proximity (or overlap) does not necessarily indicate coherence.

The coherence analysis is repeated at the same frequencies for AB power in Fig. 6. The low coherence values along the black dashed lines in Fig. 6a and b show that the AB 200 Hz lobes are less mutually coherent than the two lobes for the MIL 200 Hz case, even though the AB lobes are closer together than the MIL lobes (compare Fig. 4a and c). This further demonstrates that lobe proximity does not necessarily indicate mutual coherence, even when comparing two sets of lobes with the same acoustic wavelength. For the AB 315-Hz case, recall that no secondary lobe was present in the SPL map of Fig. 4d. The two VRs were located such that they would be incoherent. This is demonstrated in Fig. 6c and d, where coherence values are near zero along the black lines.

American Institute of Aeronautics and Astronautics
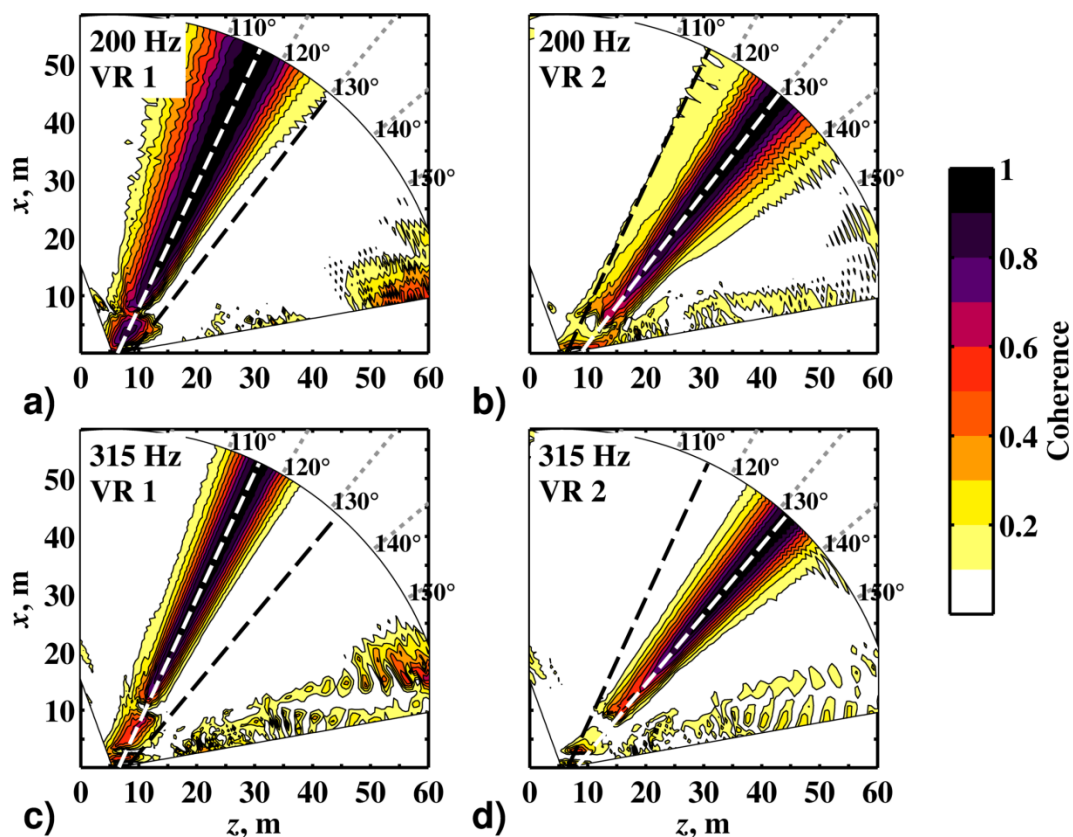
Figure 6. Coherence with respect to the selected VRs, AB power. Band center frequencies and VR numbers are shown in the upper left corners of each field. Contour lines are separated by values of 0.1. Dashed lines are placed in identical locations between left and right figures to provide a spatial reference.

As it has been established that the lobes are essentially independent, they can be isolated in the PCD procedure. The PFs that result from the PCD are shown in order to study the lobes independently. Figure 7a and b show the two PFs for MIL power at 200 Hz. Note that PF 1 is dominated by lobe 1, and PF 2 by lobe 2. However, Fig. 7a shows that PF 1 has a secondary local maximum region aft of the primary lobe; the maximum level of this region is approximately 8 dB below the maximum of the primary lobe. It is not certain if PF 1 results from a radiator with a self-coherent interference pattern, or if the pattern is an artifact of NAH projection. Certainly, the cross-talk between the VRs for the MIL 200-Hz case (see Fig. 5a) complicates the lobe isolation process. Cross-talk, or nonzero coherence, results in off-diagonal terms in the decomposed VR cross-spectral matrix. This means that potentially independent partial sources are not fully isolated in the PCD. It is important to understand that, because of this, the order of the VRs matters in the PCD process. Switching to a VR order of 2 then 1 would produce slightly different PFs that those in Fig. 7a and b (not simply the same PFs in a different order). This is because the PCD process effectively extracts all field energy that is coherent with the first VR, subtracts it from the total, and then repeats the process for the second VR. Thus, any energy that is coherent across both VRs is always represented in the first PF, not in the second.

Since two references are inadequate to capture all of the mutually independent partial sources of jet noise at these frequencies, it is helpful to know how much energy is not represented in the two PFs. To this end, Fig. 7c shows the energy from the total MIL 200-Hz field minus the energy contained in PF 1 and 2, called the residual. The regions of high amplitude at about 123° and 143° in Fig. 7a and b, respectively, correspond to null regions of Fig. 7c, particularly in the far field where the VRs were located. This is because the majority of the lobe energies are extracted from the total field. There are two main regions of high residual energy in Fig. 7c. Note that the high-amplitude region near 133° falls between the locations of the two lobes of PF 1 and PF 2. Thus, there is significant energy between the two primary lobes that was not captured by either VR.

American Institute of Aeronautics and Astronautics
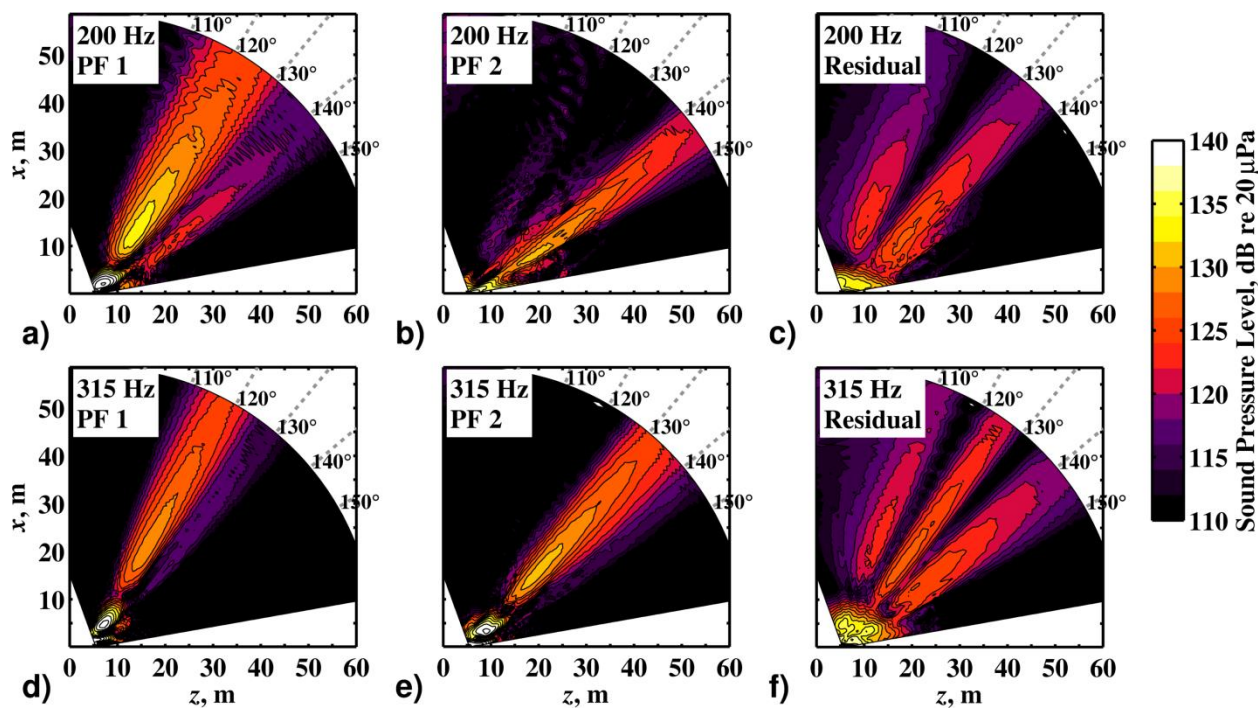
Figure 7. PFs at MIL power, 200 Hz and 315 Hz. Band-center frequencies and PF numbers are shown in the upper left corners of each field. Contour lines are separated by 2 dB.

The MIL 315-Hz case shows a similar behavior in Fig. 7d-f. The two PFs of Fig. 7d and e correspond to the null regions of Fig. 7f, outside of which are three regions of high residual amplitude, including a narrow region near 127˚, between the two lobes. Such is also the case for the AB 200-Hz and 315-Hz fields in Fig. 8 (although the PF 2 lobe for AB 315 Hz in Fig. 8e cannot be distinguished in the total SPL map of Fig. 4d). In the double-lobe cases of MIL 200 Hz, MIL 315 Hz, and AB 200 Hz, the maxima of the PF 1 and PF 2 lobes are 2-6 dB higher than the maxima of the residual between them, which allows the lobes to be visible in the total SPL map.

In order to investigate the spatial distributions of the partial sources that generate the lobes, Fig. 9 shows the PF reconstructions along the equivalent nozzle lip line. For example, Fig. 9a shows the two PF source reconstructions, the total source reconstruction, and the residual for the MIL 200-Hz case. (All source reconstructions have been truncated to the regions where reconstruction error is estimated to be less than 2 dB, as explained by Wall *et al.*[7]) Note that the maximum for PF 1 occurs at $z = 5$ m, which is near the maximum for PF 2 at $z = 6$ m. The highest 10 dB of the PF 1 distribution spans about $z = 2$ m to greater than $z = 7$ m, the highest 10 dB of PF 2 spans $z = 1$ to greater than $z = 7$ m, and the residual spans a similar region. All remaining cases in Fig. 9b-d show that the two PF source maxima occur within 1-2 m, and that the distributions of the two PFs and the residual span similar regions. Thus, the lobes that are distinct in the radiated field originate from mutually incoherent, yet spatially coincident, partial sources. Since the lobes have different angles of maximum radiation, this representation suggests overlapping, mutually incoherent sources that radiate with different characteristic phase speeds.

10
American Institute of Aeronautics and Astronautics
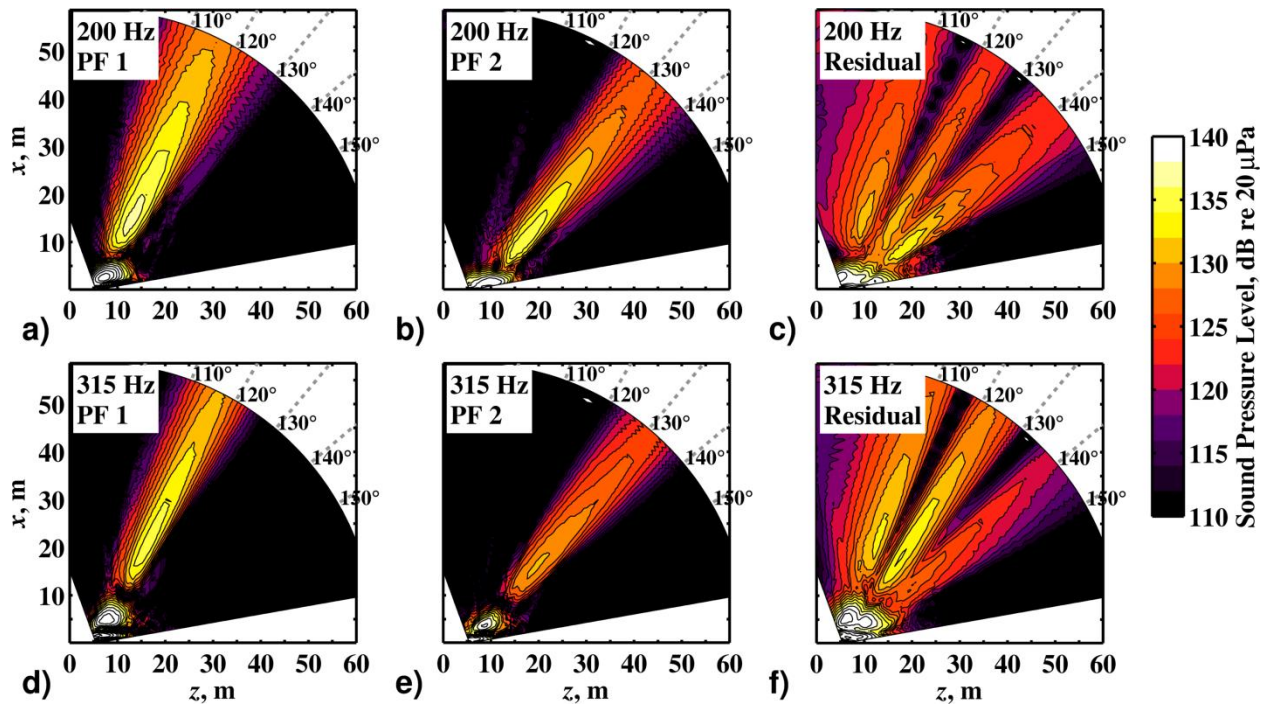
Figure 8. PFs at AB power, 200 Hz and 315 Hz. Band-center frequencies and PF numbers are shown in the upper left corners of each field. Contour lines are separated by 2 dB.
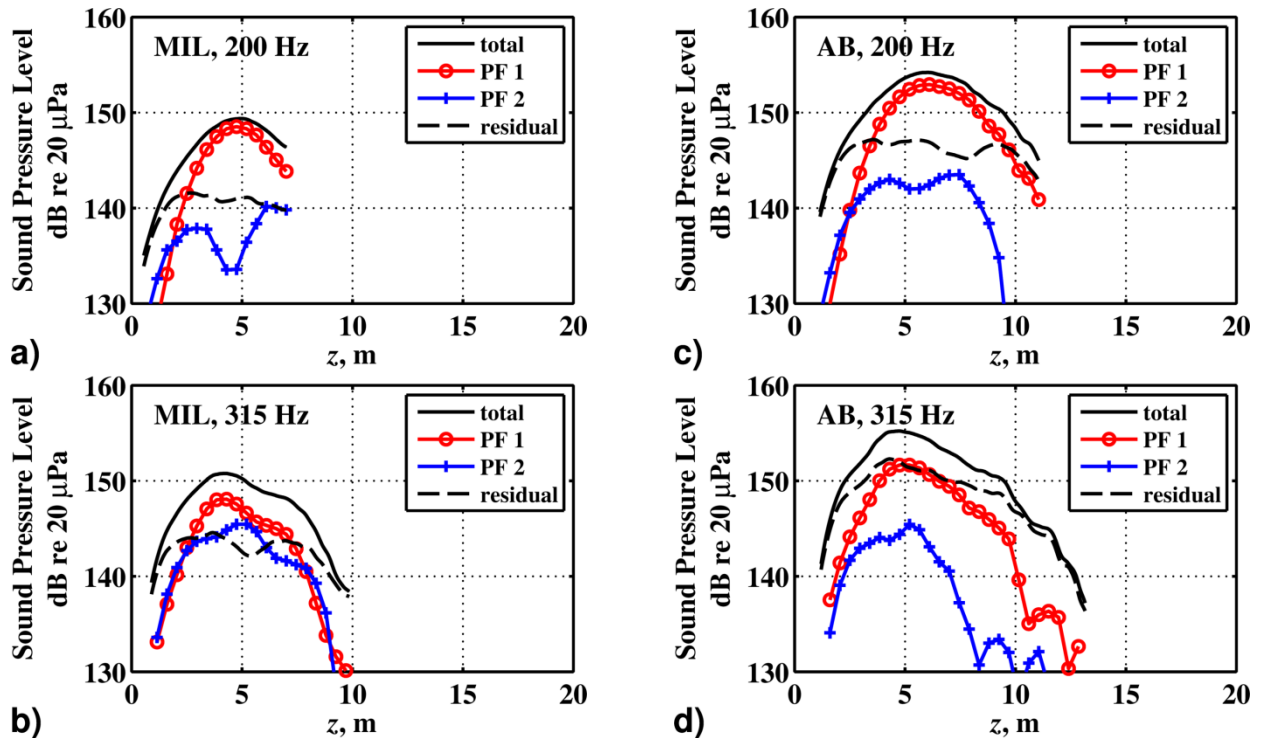
Figure 9. Total source and partial source reconstructions for (a) MIL 200 Hz, (b) MIL 315 Hz, (c) AB 200 Hz, and (d) AB 315 Hz. Partial sources are represented by the PF SPLs along the equivalent nozzle lip line. Residual levels are shown by dashed lines.

Although overlapping independent sources with variable wave speeds does provide a possible explanation for multiple lobes, it does not necessarily indicate that the lobes should be separated by the null regions that lead to the double spectral peaks of tactical aircraft jet noise. It is likely that the mixing noise from partially coherent structures in any jet could be thus represented, such as was presented by Wall *et al.*[25] for the F-22A operating at MIL power and at 400 Hz. The question remains, *What causes the dip in the radiation directivity between two independent lobes?* The answer to this question is difficult to obtain without a detailed measurement of the flow structures. However, an analogy might be made to the broadband shock-associated noise (BBSN) study by Long,[45] who used NAH to reconstruct source distributions and far-field radiation of an underexpanded jet. He showed spectral/spatial field maps that had multiple lobe patterns (striations) similar to those shown for the F-22A in Fig. 2 and by Wall *et al.*[18] The BBSN source reconstructions coincided with shadowgraph images of shock cells, and their directivity patterns agreed with previous theory of radiation from turbulent interactions with shock cell boundaries.[46,47] For the mixing noise of full-scale tactical jets, it is understood that the sources are long, partially coherent, and radiate over a range of directivity angles. It is also understood that jets from tactical aircraft engines operating on the ground are underexpanded and exhibit regularly spaced shock cells (visible in the luminescent portions of the jets in photographs[10]). Regular arrays of coherent sources can exhibit radiation patterns of constructive and destructive interference, depending on the relations between source phase speed and acoustic phase speed. It is therefore hypothesized that spatially coherent, large turbulence structures, when passing through a shock-cell region, interact with the regularly spaced variations in such a way that radiation toward some angles is less efficient than in others, leading to distinct lobes separated by shallow null regions.

V.   Concluding Discussion

In this paper, multiple, distinct lobes of jet noise radiation from an F-22A Raptor have been investigated for their mutual coherence. The fields for the engine powers and frequencies that exhibit double lobes have been reconstructed using near-field acoustical holography (NAH). Since the two lobes are highly independent, a partial coherence decomposition (PCD) method has been used to isolate their respective contributions to the total field. The partial sources that result from the decomposed fields at the equivalent nozzle lip line have been shown in order to demonstrate their respective radiation characteristics.

The partial fields (PFs), represented in this manner, show that the two lobes are generated by overlapping yet mutually incoherent partial sources in the mixing region. The different preferred angles of radiation from the coincident sources suggest that each partial source has a characteristic phase speed. This partial source representation is not unique, but the PCD based on the placement of virtual references (VRs) at the lobe centers in the far field lends physical insight into the source distributions that generate each lobe. An alternative VR placement approach, such as placement along the source region, could provide additional information about the physical sources.

Past studies showed that full-scale jet noise fields could be represented with a set of mutually incoherent, narrow lobes with variable preferred angles of radiation.[25] Here, for engine powers and frequencies with two distinct lobes, it has been shown that there exists significant acoustic energy in the null region dividing the two lobes that is not coherent with the energy in the lobe on either side. It has been hypothesized that the interactions between mixing noise sources and regularly spaced shock cells could result in less efficient radiation in certain directions, resulting in a directivity null. This explanation has some similarities to the radiation patterns that result from broadband shock-associated noise (BBSN).

One purpose of the current investigation has been to identify differences between non-afterburner and afterburner jet sources. Based on the results shown, minor differences in partial source distributions, coherences, and radiation directionalities are evident, but no qualitative difference exists—the addition of thrust in the afterburner process does not qualitatively change the nature of the sources that have been investigated here.

In future work, wavepacket models[48,49] of full-scale jet PFs will be generated and combined to provide overall field predictions, including the effects of partial coherence and multiple lobes. Future PCD work that includes additional frequencies and more complete VR sets may elucidate differences between non-afterburner and afterburner acoustic sources. The sparsely chosen frequencies of the current paper make it difficult to establish trends in the relationships between source location, extent, and lobe directivity. However, Harker *et al.*[24] showed that F-22A sound waves arriving farther downstream along a linear ground array tended to radiate in farther aft directions (at larger angles with respect to the jet inlet axis), based on an estimation of local phase speed. In future work, a similar analysis will be performed to link characteristic source phase speeds to source locations and directivities, using PFs obtained from additional PCD analyses.

American Institute of Aeronautics and Astronautics

Acknowledgments

References

[1]Schlinker, R. H., Liljenberg, S. A., Polak, D. R., Post, K. A., Chipman, C. T., and Stern, A. M., "Supersonic Jet Noise Source Characteristics & Propagation: Engine and Model Scale," *13th AIAA/CEAS Aeroacoustics Conference*, AIAA Paper 2007-3623, May 2007.

[2]Gee, K. L., Sparrow, V. W., James, M. M., Downing, J. M., Hobbs, C. M., Gabrielson, T. B., and Atchley, A. A., "The Role of Nonlinear Effects in the Propagation of Noise from High-power Jet Aircraft," *Journal of the Acoustical Society of America*, Vol. 123, No. 6, 2008, pp. 4082-4093.

[3]Neilsen, T. B., Gee, K. L., Wall, A. T., and James, M. M., "Similarity Spectra Analysis of High-performance Jet Aircraft Noise," *Journal of the Acoustical Society of America*, Vol. 133, No. 4, 2013, pp. 2116 – 2125.

[4]Gee, K. L., Gabrielson, T. B., Atchley, A. A., and Sparrow, V. W., "Preliminary Analysis of Nonlinearity in Military Jet Aircraft Noise Propagation," *AIAA Journal,* Vol. 43, No. 6, 2005, pp. 1398-1401.

[5]Greska, B., and Krothapalli, A., "On the Far-field Propagation of High-speed Jet Noise," *Proceedings of NCAD / NoiseCon 2008*, NCAD2008-73071, American Society of Mechanical Engineers, 2008.

[6]Gee, K. L., Downing, J. M., James, M. M., McKinley, R. C., McKinley, R. L., Neilsen, T. B., and Wall, A. T., "Nonlinear Evolution of Noise from a Military Jet Aircraft During Ground Run-up," *18th AIAA/CEAS Aeroacoustics Conference,* AIAA Paper 2012-2258, June 2012.

[7]Wall, A. T., Gee, K. L., Neilsen, T. B., McKinley, R. L., and James, M. M., "Military Jet Noise Source Imaging Using Multisource Statistically Optimized Near-field Acoustical Holography," *Journal of the Acoustical Society of America*, (submitted for publication).

[8]Norum, T. D., Garber, D. P., Golub, R. A., Santa Maria, O. L., and Orme, J. S., "Supersonic Jet Exhaust Noise at High Subsonic Flight Speed," NASA/TP-2004-212686, 2004.

[9]McInerny, S. A., Gee, K. L., Downing, J. M., and James, M. M., "Acoustical Nonlinearities in Aircraft Flyover Data," *13th AIAA/CEAS Aeroacoustics Conference,* AIAA Paper 2007-3654, May 2007.

[10]James, M. M., Salton, A. R., Downing, M. D., Gee, K. L., Neilsen, T. B., Reichman, B. O., McKinley, R. L., Wall, A. T., and Gallagher, H. L., "Acoustic Emissions from F-35A and F-35B Aircraft During Ground Run-Up," *21st AIAA/CEAS Aeroacoustics Conference,* AIAA Paper 2015-2375, June 2015.

[11]Greska, B., "Supersonic Jet Noise and its Reduction Using Microjet Injection," Ph.D. Dissertation, Dept. of Mechanical Engineering, The Florida State Univ., Tallahassee, FL, 2005.

[12]Neilsen, T. B., Gee, K. L., and James, M. M., "Spectral Characterization in the Near and Mid-field of Military Jet Aircraft Noise," *19th AIAA/CEAS Aeroacoustics Conference,* AIAA Paper 2013-2191, May 2013.

[13]Neilsen, T. B., Gee, K. L., Wall, A. T., James, M. M., and Atchley, A. A., "Comparison of Supersonic Full-scale and Laboratory-scale Jet Data and the Similarity Spectra for Turbulent Mixing Noise," *Proceedings of Meetings on Acoustics,* Vol. 19, Paper 040071, 2013.

[14]Tam, C. K. W., Golebiowsky, M., and Seiner, J. M., "On the Two Components of Turbulent Mixing Noise from Supersonic Jets," *2nd AIAA/CEAS Aeroacoustics Conference,* AIAA Paper 96-1716, May 1996.

[15]Tam, C. K. W., and Parrish, S. A., "Noise of High-performance Aircrafts at Afterburner," *20th AIAA/CEAS Aeroacoustics Conference,* AIAA Paper 2014-2754, June 2014.

[16]Stout, T. A., Gee, K. L., Neilsen, T. B., Wall, A. T., and James, M. M., "Intensity Analysis of the Dominant Frequencies of Military Jet Aircraft Noise," *Proceedings of Meetings on Acoustics,* Vol. 20, Paper 040010, 2014.

[17]Harker, B. M., Gee, K. L., Neilsen, T. B., Wall, A. T., and James, M. M., "Phased-array Measurements of Full-scale Military Jet Noise," *AIAA Journal* (submitted for publication).

[18]Wall, A. T., Gee, K. L., James, M. M., Bradley, K. A., McInerny, S. A., and Neilsen, T. B., "Near-field Noise Measurements of a High-performance Military Jet Aircraft," *Noise Control Engineering Journal,* Vol. 60, No. 4, 2012, pp. 421-434.

[19]Stout, T. A., Gee, K. L., Neilsen, T. B., Wall, A. T., and James, M. M., "Acoustic Intensity Near a High-powered Military Jet Aircraft," *Journal of the Acoustical Society of America* (submitted for publication).

[20]Fisher, M. J., Harper-Bourne, M., Glegg, S. A. L., "Jet Engine Noise Source Location: The Polar Correlation Tetechnique," *Journal of Sound and Vibration,* Vol. 51, No. 1, 1977, pp. 23-54.

[21]Brooks, T. F., and Humphreys Jr., W. M., "Extension of DAMAS Phased Array Processing for Spatial Coherence Determination (DAMAS-C)," *12th AIAA/CEAS Aeroacoustics Conference,* AIAA Paper 2006-2654, May 2006.

[22]Maynard, J. D., Williams, E. G., and Lee, Y., "Nearfield Acoustic Holography: I. Theory of Generalized Holography and the Development of NAH," *Journal of the Acoustical Society of America,* Vol. 78, No. 4, 1985, pp. 1395–1413.

[23]Wall, A. T., Gee, K. L., and Neilsen, T. B., "Multisource Statistically Optimized Near-field Acoustical Holography," *Journal of the Acoustical Society of America,* Vol. 137, No. 2, 2015, pp. 963-975.

[24]Harker, B. M., Neilsen, T. B., Gee, K .L., Wall, A. T., and James, M. M., "Spatiotemporal Correlation Analysis of Jet Noise from a High-Performance Military Aircraft," *21st AIAA/CEAS Aeroacoustics Conference,* AIAA Paper 2015-2376, June 2015.

[25]Wall, A. T., Gee, K. L., Neilsen, T. B., and James, M. M., "Acoustical Holography and Proper Orthogonal Decomposition Methods for the Analysis of Military Jet Noise," *Proceedings of Noise-Con 2013*, Institute of Noise Control Engineering, 2013.

[26]Kwon, H.-S., and Bolton, J. S., "Partial Field Decomposition in Nearfield Acoustical Holography by the Use of Singular Value Decomposition and Partial Coherence Procedures," *Proceedings of Noise-Con 98*, Institute of Noise Control Engineering, Poughkeepsie, NY, 1998, pp. 649-654.

[27]Veronesi, W. A., and Maynard, J. D., "Digital Holographic Reconstruction of Sources with Arbitrarily Shaped Surfaces," *Journal of the Acoustical Society of America,* Vol. 85, No. 2, 1989, pp. 588-598.

[28]Hald, J., "STSF—A Unique Technique for Scan-based Nearfield Acoustical Holography Without Restriction on Coherence," Technical Report No. 1, Bruel & Kjaer, Naerum, Denmark, 1989.

[29]Moon, T. K., and Stirling, W. C., *Mathematical Methods and Algorithms for Signal Processing*, Prentice-Hall, Upper Saddle River, NJ, 2000, pp. 275-285.

[30]Johnson, D. H., and Dudgeon, D. E., A*rray Signal Processing: Concepts and Techniques,* Prentice-Hall, Upper Saddle River, NJ, 1993.

[31]Lee, M., and Bolton, J. S., "Source Characterization of a Subsonic Jet by Using Near-field Acoustical Holography," *Journal of the Acoustical Society of America,* Vol. 121, No. 2, 2007, pp. 967-977.

[32]Long, D. F., "Jet Noise Source Location via Acoustic Holography and Shadowgraph Imagery," *14th AIAA/CEAS Aeroacoustics Conference,* AIAA Paper 2008-2888, May 2008.

[33]Vold, H., Shah, P. N., Davis, J., Bremner, P. G., McLaughlin, D., Morris, P., Veltin, J., and McKinley, R., "High-resolution Continuous Scan Acoustical Holography Applied to High-speed Jet Noise," *16th AIAA/CEAS Aeroacoustics Conference,* AIAA Paper 2010-3754, June 2010.

[34]Wall, A. T., Gee, K. L., Neilsen, T. B., Krueger, D. W., "Cylindrical Acoustical Holography Applied to Full-scale Jet Noise," *Journal of the Acoustical Society of America*, Vol. 136, No. 3, 2014, pp. 1120-1128.

[35]Nam, K.-U., and Kim, Y.-H., "Visualization of Multiple Incoherent Sources by the Backward Prediction of Near-Field Acoustic Holography," *Journal of the Acoustical Society of America,* Vol. 109, No. 5, 2001, pp. 1808–1816.

[36]Kim, Y.-J., Bolton, J. S., and Kwon, H.-S., "Partial Sound Field Decomposition in Multireference Near-field Acoustical Holography by Using Optimally Located Virtual References," *Journal of the Acoustical Society of America,* Vol. 115, No. 4, 2004, pp. 1641–1652.

[37]Wall, A. T., Gee, K. L., Neilsen, T. B., and James, M. M., "Partial Field Decomposition of Jet Noise Sources Using Optimally Located Virtual Reference Microphones," *Proceedings of Meetings on Acoustics,* Vol. 18, Paper 045001, 2012.

[38]Lee, M., and Bolton, J. S., "Scan-based Near-field Acoustical Holography and Partial Field Decomposition in the Presence of Noise and Source Level Variation," *Journal of the Acoustical Society of America,* Vol. 119, No. 1, 2006, pp. 382-393.

[39]Wall, A. T., Gee, K. L., Gardner, M. D., Neilsen, T. B., and James, M. M., "Near-field Acoustical Holography Applied to High-performance Jet Aircraft Noise," *Proceedings of Meetings on Acoustics,* Vol. 9, Paper 040009, 2012.

[40]Wall, A. T., Gardner, M. D., Gee, K. L., and Neilsen, T. B., "Coherence Length as a Figure of Merit in Multireference Near-field Acoustical Holography," *Journal of the Acoustical Society of America*, Vol. 132, No. 3, 2012, pp. EL215-EL221.

[41]Price, S. M., and Bernhard, R. J., "Virtual Coherence: A Digital Signal Processing Technique for Incoherent Source Identification," *Proceedings of the 4th International Modal Analysis Conference*, Vol. II, Union College, Schenectady, NY, 1986, pp. 1256-1262.

[42]Bendat, J. S., and Piersol, A. G., *Random Data: Analysis and Measurement Procedures*, 2nd Ed., John Wiley & Sons, New York, 1986, pp. 136-137.

[43]Tam, C. K. W., "Mach Wave Radiation from High-speed Jets," *AIAA Journal*, Vol. 47, No. 10, 2009, pp. 2440-2448.

[44]Tinney, C. E., Glauser, M. N., and Ukeiley, L. S., "Low-dimensional Characteristics of a Transonic Jet. Part 1. Proper Orthogonal Decomposition," *Journal of Fluid Mechanics*, Vol. 612, pp. 107-141.

[45]Long, D. F., "Jet Noise Source Location via Acoustic Holography and Shadowgraph Imagery," *14th AIAA/CEAS Aeroacoustics Conference,* AIAA Paper 2008-2888, May 2008.

[46]Harper-Bourne, M., and Fisher, M., "The Noise from Shock Waves in Supersonic Jets," Agard CP #131, 1973, pp. 11.1-11.13.

[47]Long, D., "The Structure of Shock Cell Noise from Supersonic Jets," *11th AIAA/CEAS Aeroacoustics Conference,* AIAA Paper 2005-2840, May 2005.

[48]Papamoschou, D., "Wavepacket Modeling of the Jet Noise Source," *17th AIAA/CEAS Aeroacoustics Conference,* AIAA Paper 2011-2835, June 2011.

[49]Jordan, P., and Colonius, T., "Wave Packets and Turbulent Jet Noise," *Annual Review of Fluid Mechanics*, Vol. 45, 2013, pp. 173-95.